Title

Induction of apoptosis by 9,10-dimethyl-1,2-benzanthracene in cultured preovulatory rat follicles is preceded by a rise in reactive oxygen species and is prevented by glutathione

Journal

Biology of Reproduction, 77(3)

ISSN

0006-3363

Authors

Tsai-Turton, M
Nakamura, BN
Luderer, U

Publication Date

2007-09-01

DOI

10.1095/biolreprod.107.060368

BIOLOGY OF REPRODUCTION **77,** 442–451 (2007)
Published online before print 6 June 2007.
DOI 10.1095/biolreprod.107.060368

Induction of Apoptosis by 9,10-Dimethyl-1,2-Benzanthracene in Cultured Preovulatory Rat Follicles Is Preceded by a Rise in Reactive Oxygen Species and Is Prevented by Glutathione[1]

Miyun Tsai-Turton,[3] Brooke N. Nakamura,[4] and Ulrike Luderer[2,3,4,5]

Departments of Community and Environmental Medicine,[3] Medicine,[4] and Developmental and Cell Biology,[5] University of California Irvine, Irvine, California 92617

ABSTRACT

The polycyclic aromatic hydrocarbon (PAH) 9,10-dimethyl-1,2-benzanthracene (DMBA) destroys primordial, primary, and secondary ovarian follicles in rodents, but its effects on antral follicles have received limited attention. PAHs are metabolized to reactive species, some of which can undergo redox cycling to generate reactive oxygen species (ROS). We previously showed that ROS initiate apoptosis in preovulatory follicles cultured without gonadotropin support and that glutathione (GSH) depletion induces apoptosis in the presence of gonadotropins. In the present study, we tested the hypothesis that DMBA induces apoptosis in preovulatory follicles, which is mediated by ROS and prevented by GSH. Preovulatory follicles were isolated from ovaries of 25-day-old rats 48 h after the injection of 10 IU of eCG and were cultured with DMBA in the presence of FSH for 2 to 48 h. DMBA induced granulosa cell (GC) and theca cell (TC) apoptosis at 48 h, as judged by TUNEL and activated caspase-3 immunostaining. DMBA treatment also increased the numbers of GCs and TCs that immunostained for the proapoptotic protein BAX. Follicular ROS levels were significantly increased in DMBA-treated follicles at 12, 24, and 48 h. GSH supplementation protected against and GSH depletion enhanced the induction of apoptosis in GCs and TCs by DMBA. These findings suggest that GSH is a critical protective mechanism against DMBA-induced apoptosis in antral follicles and that ROS generation may mediate DMBA-induced GC apoptosis.

apoptosis, atresia, dimethylbenzanthracene, follicle, glutathione, oxidative stress, polycyclic aromatic hydrocarbon, toxicology

INTRODUCTION

Polycyclic aromatic hydrocarbons (PAHs) are ubiquitous environmental toxicants that are formed during incomplete combustion and carbonization of organic materials [1]. Humans are exposed to PAHs through work in the production, refining, and use of coal, oil shale, or mineral oil [1, 2] and through ambient air pollution, tobacco smoke, and foods [3]. PAHs are carcinogens and ovarian toxicants. Studies in mice and rats have shown that the PAHs 9,10-dimethyl-1,2-benzanthracene (also called 7,12-dimethylbenz[a]anthracene; DMBA), 3-methylcholanthrene (3-MC), and benzo[a]pyrene (BaP) destroy ovarian follicles [4–7]. Evidence for ovarian toxicity of PAHs in humans comes from epidemiologic studies demonstrating that women who smoke have earlier onset of menopause [8, 9] and decreased fecundity [10, 11] compared with women who do not smoke. Most rodent studies have focused on the destruction of follicles in the earliest stages of development, the primordial and primary follicles. Destruction of primordial follicles can lead to premature ovarian failure, but more acute effects on fertility, such as the decreased per menstrual cycle probability of pregnancy observed in women who smoke [11], are more consistent with destruction of follicles at later stages of development, such as secondary and antral stages. However, the effects of PAHs on larger, growing follicles have received limited attention. Destruction of antral follicles was reported 2–4 days after treatment with DMBA in mice [6]. A dramatic decline in corpora lutea numbers within 1 wk of BaP treatment in mice is also consistent with an effect on antral follicles [12].

PAHs like DMBA undergo extensive metabolism. The parent compounds themselves are not thought to be toxic. The most well-characterized pathway begins with oxidation by cytochromes P450 (primarily CYP1A1 and 1B1) to arene oxides, which can be hydrolyzed by microsomal epoxide hydrolase to dihydrodiols, which can be further oxidized to highly reactive diol epoxides by CYP1A1 and CYP1B1 [13, 14]. The diol epoxides can form DNA adducts and were long thought to be the ultimate carcinogens [15, 16] and ovotoxicants [17]. However, other metabolic products of PAHs may also mediate some of these toxic effects. The dihydrodiols can undergo metabolic activation by didydrodiol dehydrogenases to quinones [18]. The BaP quinones increase reactive oxygen species (ROS) formation in cultured cells, which may result in oxidative DNA damage [18, 19].

The tripeptide glutathione (GSH) is present at millimolar concentrations in cells and is the most abundant intracellular thiol [20]. GSH detoxifies ROS by spontaneous or GSH peroxidase-catalyzed reduction [20]. GSH-*S*-transferase-catalyzed conjugation of electrophilic toxicants with GSH is an important detoxification mechanism for many exogenous toxicants [20]. Conjugation with GSH is the primary detoxification mechanism for the diol epoxides of PAHs [21–23]. The arene oxide and quinone metabolites of PAHs also undergo GSH conjugation [1, 18]. The ovary has moderately high GSH concentrations compared with other organs [24, 25], and ovulated oocytes have among the highest GSH concentrations of any cell type (9–10 mM) [26]. GSH is necessary for normal oocyte spindle function and formation of the female

[1]Supported by NIH grant K08 ES10963 (to U.L), the University of California Irvine Developmental Biology Center and Chao Family Comprehensive Cancer Center Optical Biology Shared Resource (NIH Cancer Center Support grant P50 CA62203), and the Center for Occupational and Environmental Health, University of California, Irvine.
[2]Correspondence: Ulrike Luderer, Center for Occupational and Environmental Health, 5201 California Ave., Suite 100, Irvine, CA 92617. FAX: 949 824 2345; e-mail: uluderer@uci.edu

Received: 25 January 2007.
First decision: 15 February 2007.
Accepted: 30 May 2007.

ISSN: 0006-3363. http://www.biolreprod.org

pronucleus and for normal male pronuclear decondensation [27–29]. We have shown that ovarian GSH synthesis is regulated by gonadotropin modulation of the expression of the catalytic and modulatory subunit of the rate-limiting enzyme in GSH synthesis, glutamate cysteine ligase, in a follicle stage-dependent manner, with high levels of mRNA expression in granulosa cells (GCs) of growing follicles during most of the estrous cycle [30–32]. GSH depletion increased antral follicle atresia in vivo and in vitro [24, 33].

The mechanisms by which PAHs destroy primordial follicles in fetal and neonatal mouse ovaries appear to involve the aryl hydrocarbon receptor (AHR), a member of the Per-Arnt-Sim gene family of transcription factors, and the proapoptotic BCL2 family protein BAX. Destruction of primordial follicles by DMBA appears to be driven by apoptosis of the oocyte, with secondary death of the somatic cells, much like endogenous atresia in primordial follicles [34]. DMBA treatment upregulated BAX protein expression in primordial oocytes, and treatment with an AHR receptor antagonist blocked this destruction [35]. Moreover, ovaries from mice that lacked a functioning *Ahr* gene or a functioning *Bax* gene were resistant to DMBA-induced destruction of primordial follicles [35]. However, no studies have investigated the mechanisms by which PAHs destroy larger, growing ovarian follicles in adult rodents. Because the natural process of apoptotic follicular degeneration, which is called atresia, occurs predominantly in antral follicles and is driven by GC apoptosis [34], we hypothesized that DMBA destroys antral follicles by inducing GC apoptosis. Second, because PAH metabolites have been shown to generate ROS [18, 19], we hypothesized that the induction of apoptosis by DMBA is mediated by oxidative stress. Finally, because GSH is important in detoxifying both reactive metabolites of DMBA and ROS, we hypothesized that GSH depletion would potentiate and that GSH supplementation would prevent the induction of apoptosis by DMBA.

MATERIALS AND METHODS

Materials

All chemicals were purchased from Sigma or Fisher Scientific, unless otherwise noted. Tissue culture reagents were from Invitrogen. The eCG and ovine FSH (NIDDK-oFSH-20 in vivo biological potency of 4453 IU/mg) were obtained from Dr. A.F. Parlow, National Hormone and Peptide Program, NIDDK (National Institute of Diabetes and Digestive and Kidney Diseases). WST-1 reagent, diaminobenzidine (DAB) substrate and buffer, and In Situ Cell Death Detection Kit POD (peroxidase) were from Roche Applied Science.

Animals

Sprague-Dawley rats, 22- to 23-day-old females (Crl:CD(SD)IGS BR) weighing 40–51 g, were obtained from Charles River Laboratories. Upon arrival, two to three animals per cage were housed in an AAALAC (Association for Assessment and Accreditation of Laboratory Animal Care)-accredited facility, with free access to deionized water and standard laboratory chow, on a 14L:10D cycle. The experimental protocols were approved by the Institutional Animal Care and Use Committee at the University of California, Irvine.

Preovulatory Follicle Isolation and Culture

The 25-day-old female rats were injected subcutaneously with 10 IU of eCG in 0.1 ml of sterile 0.9% NaCl to promote growth of a cohort of follicles. Forty-eight hours after the eCG treatment, the animals were killed by carbon dioxide asphyxiation for collection of ovaries. Ovaries were placed on ice in serum-free medium pregassed with 95% O_2 and 5% CO_2. Healthy large antral (preovulatory) follicles (8–12 per ovary) between 600 and 800 μm in diameter were isolated with iris forceps and 27-gauge needles under a stereomicroscope by an aseptic technique, as previously described [33, 36, 37]. To minimize spontaneous apoptosis during follicle preparation, only one ovary was processed at one time, and isolated follicles were kept at 4°C until ready to culture.

Isolated preovulatory follicles (five to six follicles per treatment group per experiment) were cultured in sterile 20-ml glass scintillation vials in 2 ml of serum-free culture medium (MEM) consisting of Eagle Minimal Essential Medium supplemented with 2 mM L-glutamine, 100 U/ml penicillin, 100 μg/ml streptomycin sulfate, and 0.1% fatty acid-free BSA. Each vial was gassed with 95% O_2 and 5% CO_2, sealed with Vaseline, covered with Parafilm, and then incubated in a shaking water bath at 37°C for 2 to 48 h. Each vial was regassed every 12 h until the time of collection. Depending on the experiment, follicles were cultured with subsets of the following treatments: 1) 75 ng/ml ovine FSH, 2) FSH plus various concentrations of DMBA, 3) FSH plus antioxidant, 4) FSH plus 100 μM buthionine sulfoximine (BSO), 5) FSH+DMBA+BSO, or 6) FSH+DMBA plus antioxidant. BSO is a specific inhibitor of GSH synthesis [38]. The concentration of BSO was chosen to suppress follicular GSH to undetectable levels based on our previous studies in cultured preovulatory follicles [33]. The antioxidants were 5 mM GSH ethyl ester (GEE), 0.5 mM dithiothreitol (DTT), and 0.2 mM butylated hydroxytoluene (BHT). GEE is a cell-permeable analog of GSH [39]. The concentration of GEE was based on our previous study of cultured preovulatory follicles [33]. DTT is a thiol antioxidant. BHT is a phenolic antioxidant. Concentrations of DTT and BHT were chosen on the basis of previously published studies [40–42]. DMBA was dissolved in dimethylsulfoxide (DMSO). Control groups received an equal volume of DMSO alone. The final concentration of DMSO in all groups was 1% (v/v).

At the time of collection, follicles were processed for several assays as follows. For 8- and 24-h GSH and oxidized GSH (GSSG) assays, six antral follicles were immediately homogenized on ice in 54 μl of TES-SB buffer (20 mM Tris, 1 mM EDTA, 250 mM sucrose, 2 mM L-serine, and 20 mM boric acid). A 6-μl aliquot of homogenate was removed for protein assay with a bicinchoninic acid kit (Pierce); then, 12 μl of 5% sulfosalicylic acid (SSA) was added to the remaining homogenate, which was incubated on ice for 15 min and centrifuged at 14 000 × *g* for 2 min at 4°C; supernatants were then stored at −70°C. Follicles were homogenized in 65 μl of 5% SSA for 48-h GSH assays. For TUNEL and activated caspase-3 and BAX immunostaining, follicles were prefixed in 4% paraformaldehyde in PBS for 30 min at 4°C, cryopreserved in 15% sucrose in PBS for 90 min at 4°C, embedded in Tissue Tek OCT (Sakura Finetek), and stored at −70°C until sectioning at 10-μm thickness with a cryostat. For oxidative stress assessment, follicles were immediately processed for confocal laser scanning microscopy.

Total GSH and GSSG Assays

Supernatants from homogenized follicles were analyzed for total GSH and GSSG with a microplate enzymatic recycling assay, modified from Griffith [30, 31, 43]. For measurement of GSSG, reduced GSH (rGSH) was first removed from the sample by conjugation with 2-vinylpyridine, followed by chloroform extraction. For both GSH and GSSG assays, triplicates of samples or standards were combined with 33 μl of metal-free water and incubated for 10 min at 30°C. The samples were then mixed with 140 μl of 0.3 mM NADPH, 20 μl of 6 mM DTNB (5,5′-dithiobis(2-nitrobenzoic acid)), and 2 μl of 50 U/ml GSH reductase. The rate of TNB formation from DTNB was proportional to the total GSH concentration in each sample. TNB formation was monitored by measuring the absorbance at 412 nm for 5 min every 10 sec with a Molecular Devices Versamax microplate reader. The concentrations of total GSH or GSSG in the samples were calculated from a standard curve generated from the slopes of the standards. The concentration of rGSH was calculated as [total GSH] − 2 × [GSSG]. The intraassay coefficients of variation (CV) for total GSH ranged from 4.1% to 8.1% for GSH, and the interassay CV was 4.4%. The GSSG samples were all measured in a single assay for which the intraassay CV was 1.8%.

TUNEL Assay for In Situ Detection of Apoptosis

TUNEL was performed with the In Situ Cell Death Detection Kit as described [32, 33]. Briefly, sections were blocked with 3% H_2O_2 in methanol, permeabilized with 0.1% Triton X-100 in 0.1% sodium citrate, blocked with 3% BSA, and incubated with terminal deoxynucleotidyl transferase (TdT) solution with fluorescein-labeled 2′-deoxyuridine 5′-triphosphate. After washing, sections were again blocked with 3% BSA, washed, and incubated with peroxidase converter solution, followed by color development with DAB. Lastly, slides were counterstained with hematoxylin and mounted with Permount. Negative controls were treated with label solution without TdT. Positive controls were pretreated with DNase 1 (1 U/ml) prior to labeling.

For quantification of apoptosis, the numbers of TUNEL-positive GCs or theca cells (TCs) were counted in a blinded manner in five 400× fields per follicle with an Olympus BX60 microscope. The averages of the five GC

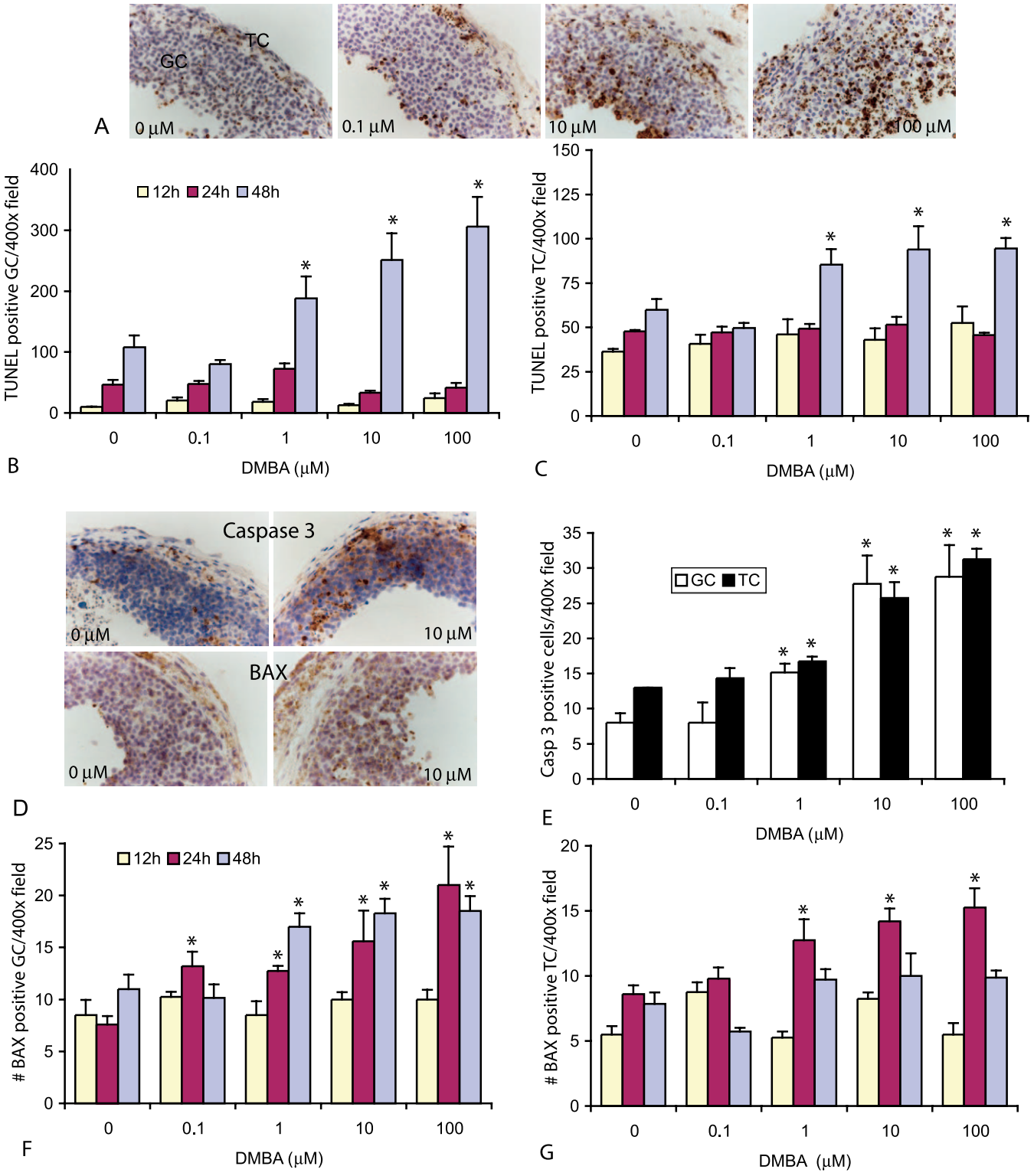

FIG. 1. DMBA treatment induces GC and TC apoptosis in cultured preovulatory follicles. Follicles were cultured for 12, 24, or 48 h with 75 ng/ml ovine FSH with 0, 0.1, 1, 10, or 100 μM DMBA and were processed for TUNEL or for activated caspase-3 or BAX immunohistochemistry as detailed in *Materials and Methods*. **A**) Representative images of follicles cultured for 48 h and processed for TUNEL. TUNEL-positive GCs and TCs are stained brown. Original magnification ×132. **B**) Mean + SEM number of TUNEL-positive GCs per ×400 field after the indicated times in culture ($N = 4$–8/group). The effect of DMBA concentration was statistically significant by the Kruskal-Wallis test at 48 h ($P < 0.001$; *significantly different from the respective 0 μM control by the Mann-Whitney test at $P < 0.05$). **C**) Mean + SEM number of TUNEL-positive TCs per ×400 field ($N = 4$–8/group). The effect of DMBA concentration was statistically significant by the Kruskal-Wallis test at 48 h ($P = 0.001$; *significantly different from the respective 0 μM control by the Mann-Whitney test at $P < 0.05$). **D**) Representative images of follicles cultured for 48 h with the indicated concentrations of DMBA and processed for activated caspase-3 immunostaining are shown at top. Activated caspase-3-positive cells are stained brown. Representative images of follicles cultured for 48 h with the indicated concentrations of DMBA and processed for BAX immunostaining are shown at bottom. BAX-positive cells are stained brown. Original magnifications ×132. **E**) Mean + SEM number of activated caspase-3-positive GCs and TCs per ×400 field after 48 h of treatment ($N = 3$–7/group). The

counts and the five TC counts were calculated for each follicle, and these values were used for statistical analyses.

Immunohistochemistry for Cleaved Caspase-3 and BAX

Immunohistochemistry was performed with a polyclonal cleaved caspase-3 antibody (1:5 dilution, Asp175, no. 9661, Cell Signaling Technology) or a polyclonal BAX antibody (1:150 dilution, 554106, BD Biosciences Pharmingen) and the Vectastain ABC Kit (Vector Laboratories), as previously described [33]. For antigen retrieval, slides were heated with a conventional microwave in 1 mM sodium citrate, and 1 mM citric acid buffer. The slides were sequentially blocked with 3% H_2O_2 in methanol, blocking serum, and avidin D/biotin blocking solution. The slides were then incubated with primary antibody overnight at 4°C, followed by biotinylated secondary antibody, ABC (avidin-biotin-horseradish peroxidase molecular complex) reagents, and DAB substrate. Finally, the slides were counterstained with hematoxylin and mounted.

The numbers of activated caspase-3 or BAX-positive GCs or TCs per 400× field were counted in five independent fields of the same follicle on two different slides. The averages were used for data analysis and presentation.

In Situ ROS Detection

ROS were detected in whole cultured follicles by laser scanning confocal microscopy with two different probes as previously described [33]. Briefly, after 2–48 h of culture, follicles were washed with PBS and incubated with 100 μM 2′,7′-dichlorofluorescein diacetate (DCF) or 100 μM dihydrorhodamine 123 (DHR; both from Molecular Probes) in MEM medium for 30 min and were washed again. DCF or DHR fluorescence was viewed and quantified with a Zeiss LSM 511 META laser scanning confocal microscope. The objective was set as Plan-Neofluor 10×/0.3, and the reflector was set as GFP (green filter). Excitation filter and tracking were configured to a single track of cy2/alexa488 fluorescein isothiocyanate, and emission filter was configured to BP-500–530. For scanning parameters, frame size of 512 × 512, scan speed of 9, and scan average of 4 were set. The Z Stack option was chosen to detect DCF or DHR fluorescence intensity in 15 evenly spaced, 10- to 25-μm-thick layers of each follicle. The mean DCF or DHR fluorescence intensity of each follicle was obtained with the Histo option, wherein the DCF or DHR intensities from all 15 layers were calculated, pooled, and averaged.

Statistical Analyses

Data from two or three replicate experiments were pooled for statistical analyses. Homogeneity of variances was assessed by the Levene test. When variances were not homogeneous, a natural logarithm transformation was applied. The differences among groups were analyzed by ANOVA followed by Fisher Least Significant Difference (LSD) test. When variances remained nonhomogeneous after data transformation, the Kruskal-Wallis test for nonparametric data was used. If the Kruskal-Wallis test was significant at $P < 0.05$, the Mann-Whitney test was then used for intergroup comparisons. Statistical analyses were carried out by SPSS 11.0 for Mac OS X.

RESULTS

DMBA-Induced Apoptosis in Cultured Preovulatory Follicles

To investigate the mechanism by which DMBA destroys antral follicles, we utilized a whole follicle culture system. Previous studies have shown that preovulatory follicles spontaneously undergo apoptosis within 24 h when cultured in the absence of gonadotropin support [44]. FSH treatment inhibits GC apoptosis in these cultured follicles [44, 45], as does gonadotropin treatment in vivo [36]. To test whether DMBA induces apoptosis in large follicles, we cultured preovulatory follicles with 75 ng/ml FSH and 0, 0.1, 1, 10, or 100 μM DMBA for 12, 24, or 48 h. DMBA treatment significantly increased the numbers of TUNEL-positive, apoptotic GCs (Fig. 1, A and B) and TCs (Fig. 1, A and C) at 48 h but not at 12 or 24 h ($P < 0.001$ and $P = 0.001$, effect of DMBA concentration by the Kruskal-Wallis test at 48 h on GC and TC apoptosis, respectively). Activated caspase-3 immunostaining paralleled the results obtained by TUNEL (Fig. 1, D and E). DMBA treatment for 48 h statistically significantly increased the numbers of activated caspase-3-positive GCs and TCs ($P = 0.002$ and $P = 0.001$, effect of DMBA concentration by the Kruskal-Wallis test on GC and TCs, respectively). DMBA treatment also caused statistically significant increases in the numbers of BAX-immunopositive GCs ($P < 0.001$, effect of concentration by two-way ANOVA) and TCs ($P < 0.001$, effect of concentration) (Fig. 1, D, F, and G). One-way ANOVAs for each time point separately showed that BAX immunostaining in GCs was significantly increased above 0 μM control levels in all DMBA-treated groups at 24 h and in 1, 10, and 100 μM groups at 48 h. TC BAX immunostaining was significantly increased above 0 μM control levels in 1, 10, and 100 μM groups at 24 h.

DMBA Did Not Alter Follicular GSH Concentrations

Conjugation with GSH is an important phase 2 biotransformation pathway for diol epoxide and other metabolites of DMBA [1, 21–23]. Reduced GSH also detoxifies ROS that may be produced as a result of PAH exposure; this results in oxidation of GSH. To determine whether treatment with DMBA depletes follicular GSH concentrations or alters the ratio of reduced GSH (rGSH) to GSSG, we measured follicular levels of total GSH and GSSG and calculated the concentration of rGSH after 8, 24, and 48 h of treatment. For the 48-h experiments, follicles were homogenized directly in 5% SSA, which precludes measuring protein concentrations in the samples. For the 8- and 24-h experiments, follicles were first homogenized in TES-SB buffer so that an aliquot of sample could be removed for protein assay prior to acidification. The results of the analyses did not differ appreciably whether GSH concentrations were expressed in nanomoles per follicle or per milligram of protein. Treatment with DMBA did not significantly alter concentrations of total GSH per follicle (Fig. 2A). DMBA treatment also did not significantly affect the rGSH or GSSG concentrations (Fig. 2, B and C). As we have previously reported [33], follicular GSH concentrations increased significantly with duration of treatment with FSH ($P < 0.001$, effect of time in culture for total GSH, rGSH, and GSSG; Fig. 2, A–C).

DMBA Increased ROS in Cultured Preovulatory Follicles

To test whether ROS are generated upon culture of preovulatory follicles with DMBA, we utilized two probes,

effect of DMBA concentration was statistically significant by the Kruskal-Wallis test ($P = 0.002$ and $P = 0.001$ for GCs and TCs, respectively; *significantly different from the respective 0 μM control by the Mann-Whitney test at $P < 0.05$). **F**) Mean + SEM number of BAX-immunopositive GCs per ×400 field after 12, 24, or 48 h of treatment ($N = 4$–5 follicles/group). There were statistically significant effects of DMBA concentration ($P < 0.001$ by two-way ANOVA), treatment duration ($P < 0.001$), and concentration × duration interaction ($P = 0.004$) on the natural log-transformed number of BAX-positive GCs. **G**) Mean + SEM number of BAX-immunopositive TCs per ×400 field after 12, 24, or 48 h of treatment ($N = 4$–5 follicles/group). There were statistically significant effects of DMBA concentration ($P < 0.001$), treatment duration ($P < 0.001$), and concentration × duration interaction ($P = 0.002$) on the number of BAX-positive TCs. *Significantly different from the respective 0 μM control levels by the LSD test at $P < 0.05$.

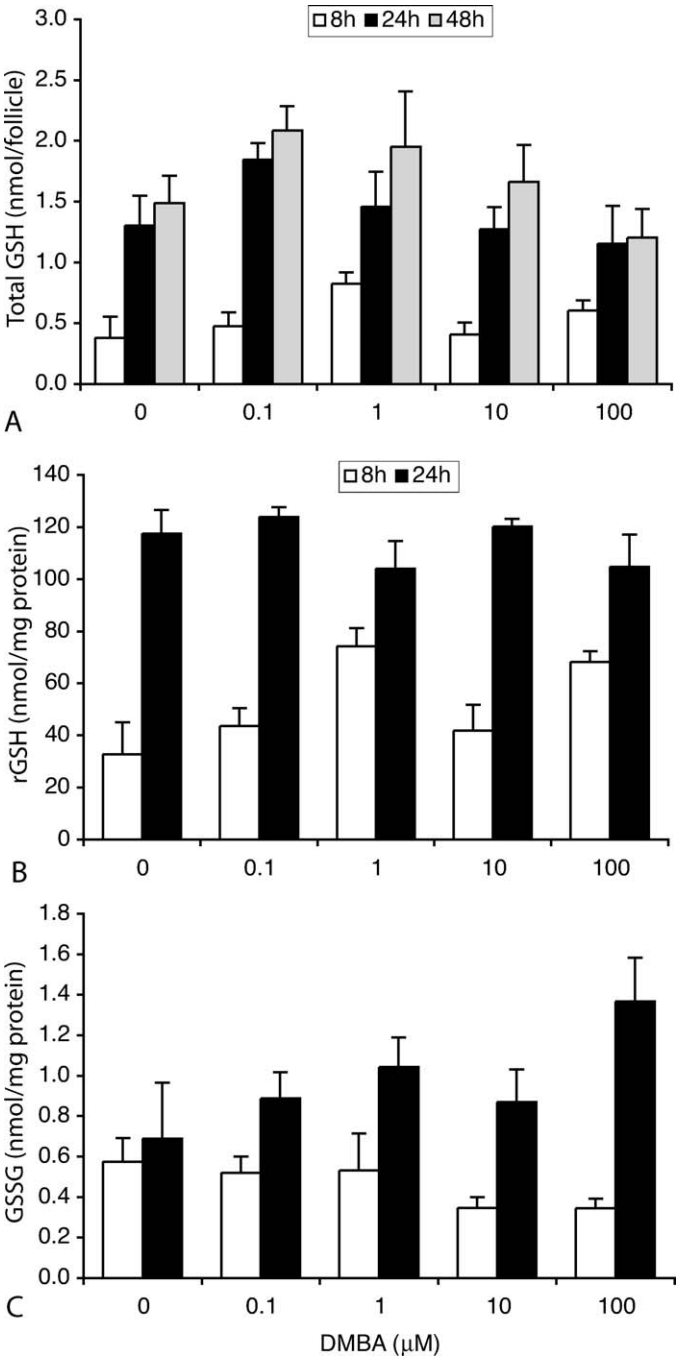

FIG. 2. DMBA treatment does not significantly alter follicular concentrations of total glutathione, reduced glutathioine (rGSH), or oxidized GSH (GSSG). Preovulatory follicles were cultured as for Figure 1 for 8, 24, or 48 h. Follicles were then processed for assay of total GSH and GSSG concentrations as described in *Materials and Methods*. Reduced GSH was calculated as [total GSH] − (2 × [GSSG]). **A**) Mean + SEM of total follicular GSH concentration in nanomoles per follicle. **B**) Mean + SEM rGSH in nanomoles per milligram of protein. **C**) Mean + SEM GSSG in nanomoles per milligram of protein. The effects of DMBA concentration on total GSH, rGSH, and GSSG were not statistically significant by two-way ANOVA. The effect of time in culture was statistically significant for total GSH, rGSG, and GSSG ($P < 0.001$). $N = 4$–5 sets of six follicles each/group.

2′,7′-DCF and DHR 123, which are oxidized to fluorescent compounds in the presence of ROS [46, 47].

Preovulatory follicles were cultured with 0, 0.5, 1, and 10 μM DMBA in the presence of 75 ng/ml FSH. Additional groups of follicles were cultured without FSH in MEM medium alone as positive controls for the generation of ROS [33]. As expected, both DCF and DHR fluorescence increased markedly by 12 h of culture in MEM and remained elevated above 0-h levels thereafter ($P < 0.001$ and $P = 0.004$ effect of time for DCF [Fig. 3A] and DHR [Fig. 3B], respectively, by the Kruskal-Wallis test). To assess the effects of DMBA concentration and treatment duration on ROS generation, two-way ANOVAs were performed, excluding the positive control MEM group. There were statistically significant effects of both DMBA concentration ($P = 0.004$) and treatment duration ($P < 0.001$) on DCF fluorescence intensity, with greater concentrations of DMBA leading to greater DCF fluorescence (Fig. 3A). DCF fluorescence was significantly increased above 0-h control levels by 12 h in the 1 and 10 μM groups and by 24 h in the 0.5 μM group. The trends were similar for DHR fluorescence, which increased with both DMBA concentration and treatment duration (Fig. 3B). The effects of treatment duration ($P < 0.001$) and DMBA concentration × duration interaction ($P = 0.037$) were statistically significant, and the effect of DMBA concentration alone approached significance ($P = 0.072$). Because the DHR data were nonhomogeneous, even after transformation, the Kruskal-Wallis tests were also performed. The effect of treatment duration was statistically significant for all concentrations of DMBA ($P < 0.05$) but not for the 0 μM group cultured with FSH alone ($P = 0.212$), again consistent with increased ROS generation upon culture with DMBA. DHR fluorescence was significantly increased above 0-h levels in the 1 and 10 μM groups by 24 h ($P < 0.01$ by the Mann-Whitney test).

Supplementation of GSH Protects Against DMBA-Induced Apoptosis

To test whether the increase in ROS mediates DMBA-induced apoptosis, we cotreated preovulatory follicles with 75 ng/ml FSH and 10 μM DMBA in the presence or absence of one of three antioxidants, GEE, DTT, or BHT. Follicular apoptosis was assessed by TUNEL and activated caspase-3 immunostaining.

Treatment with 10 μM DMBA for 48 h induced significant increases in GC and TC apoptosis as assessed by TUNEL ($P = 0.002$ and $P < 0.001$, effect of treatment on GC and TC apoptosis, respectively; Fig. 4A). The increased GC and TC apoptosis was completely prevented by cotreatment with GEE ($P < 0.01$, FSH+DMBA+GEE versus FSH+DMBA by LSD test). The effects on GCs were similar when apoptosis was assessed by activated caspase-3 immunostaining ($P = 0.001$, effect of treatment on GC apoptosis by Kruskal-Wallis test; Fig. 4B). Treatment with DMBA increased GC apoptosis by 2-fold compared with FSH alone, although the intergroup comparison was not statistically significant. Cotreatment with GEE completely prevented the increase in activated caspase-3 immunostaining. Cotreatment with two other antioxidants, DTT and BHT, did not protect against DMBA-induced GC and TC apoptosis. In fact, these agents induced significant GC and TC apoptosis, even in the absence of DMBA, compared with FSH alone (Fig. 4, A and B).

GSH Depletion Potentiates the Proapoptotic Effect of DMBA in Cultured Preovulatory Follicles

Because GSH conjugation is an important detoxification mechanism for metabolites of DMBA and for ROS, we hypothesized that GSH depletion would sensitize follicles to the induction of apoptosis by DMBA. To test this hypothesis,

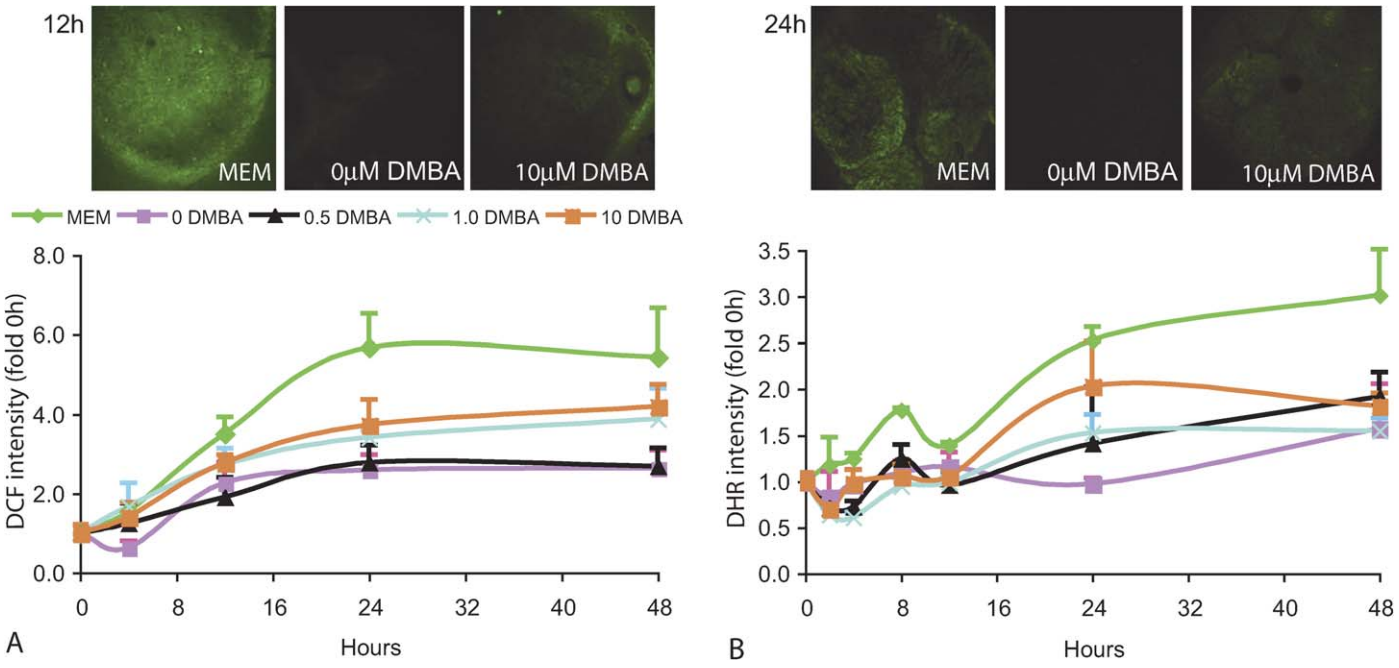

FIG. 3. Treatment with DMBA increases reactive oxygen species (ROS) generation in cultured follicles. Preovulatory follicles were cultured and treated with FSH plus 0, 0.5, 1, or 10 μM DMBA for various lengths of time ranging from 0 to 48 h. Additional groups of follicles were cultured in MEM medium alone without FSH as positive controls for the generation of ROS. At the end of the treatment periods, follicles were incubated with 2′,7′-dichlorofluorescein diacetate or dihydrorhodamine 123, and the generation of their fluorescent oxidation products, DCF and DHR, was measured by laser scanning confocal microscopy as described in *Materials and Methods*. **A**) Representative images at top show DCF fluorescence in follicles cultured for 12 h with the indicated treatments. Positive control (MEM) follicles have bright fluorescence, which was attenuated in follicles cultured with FSH (0 μM DMBA) and intermediate in follicles cultured with FSH+DMBA. The graph shows mean + SEM DCF fluorescence intensity expressed as fold 0-h control ($N = 6$ follicles/group). The effects of DMBA concentration ($P = 0.004$) and treatment duration ($P < 0.001$) were statistically significant by two-way ANOVA. DCF fluorescence in the 1 and 10 μM DMBA groups was significantly elevated above 0-h levels by 12 h ($P < 0.02$ by LSD test after one-way ANOVA within DMBA concentration group); in the 0.5 μM DMBA group, it was significantly increased by 24 h ($P < 0.01$). **B**) Representative images at top show DHR fluorescence in follicles cultured for 24 h with the indicated treatments. The graph shows mean + SEM DHR fluorescence intensity expressed as fold 0-h control ($N = 5$–6 follicles/group). The effects of treatment duration ($P < 0.001$) and duration × DMBA concentration interaction ($P = 0.037$) were statistically significant. The effect of DMBA concentration approached significance ($P = 0.072$). Kruskal-Wallis tests showed significant effects of treatment duration for all DMBA concentrations ($P < 0.05$) but not for the 0 μM DMBA groups cultured with FSH alone. DHR fluorescence in the 1 and 10 μM DMBA groups was significantly elevated above 0-h levels by 24 h ($P < 0.01$ by the Mann-Whitney test).

we cultured follicles with 75 ng/ml FSH with or without BSO, a specific inhibitor of GSH synthesis, for 8 h to allow follicular GSH concentrations to fall prior to adding DMBA for an additional 40 h of culture [33]. We chose a concentration of DMBA, 0.5 μM, which was not expected to induce GC apoptosis alone based on the data presented in Figure 1.

Follicular GSH was suppressed to undetectable levels in follicles treated with FSH+BSO or with FSH+BSO+DMBA for 48 h (from 2.0 ± 0.2 nmol/follicle in FSH-treated and 1.9 ± 0.1 nmol/follicle in FSH+DMBA-treated to less than 0.04 nmol/follicle in FSH+BSO and FSH+DMBA+BSO groups). The number of TUNEL-positive, apoptotic GCs varied with treatment in a statistically significant manner ($P = 0.002$, Kruskal-Wallis test; Fig. 5A). The numbers of TUNEL-positive GCs were significantly greater in the FSH+BSO and FSH+BSO+DMBA groups than in the group cultured with FSH alone ($P = 0.023$ and $P < 0.001$, respectively, by the Mann-Whitney test). Combined treatment with BSO and DMBA caused greater GC apoptosis than either treatment alone ($P = 0.010$ and $P = 0.376$, FSH+BSO+DMBA versus FSH+DMBA and versus FSH+BSO, respectively). There was no effect of treatment on TC apoptosis ($P = 0.391$). Similar effects on GCs were observed when activated caspase-3 immunostaining was used as an indicator of apoptosis (Fig. 5B). The number of activated caspase-3-positive GCs varied with treatment in a statistically significant manner ($P = 0.004$ by the Kruskal-Wallis test). Combined treatment with BSO and DMBA again caused greater GC apoptosis than either treatment alone ($P = 0.016$ and $P = 0.286$, FSH+BSO+DMBA versus FSH+DMBA and versus FSH+BSO, respectively). In addition, combined treatment with BSO and DMBA significantly increased the number of caspase-3-positive TCs compared with either treatment alone ($P = 0.002$, overall effect of treatment; $P = 0.016$ and $P = 0.016$, FSH+BSO+DMBA versus FSH+DMBA and versus FSH+BSO, respectively).

DISCUSSION

PAHs are ubiquitous environmental toxicants that destroy ovarian follicles in rodents [4–7] and in explanted human ovarian tissue [35]. Although most attention has focused on the destruction of primordial follicles by PAHs, there is evidence that these compounds are also capable of destroying secondary and antral follicles [4, 12]. We used a well-characterized model system in which antral follicles cultured without gonadotropin support spontaneously undergo apoptosis, and gonadotropin treatment prevents apoptosis, to study the effects of DMBA on apoptosis in large antral follicles. We showed that DMBA induces GC and TC apoptosis and that the onset of apoptosis is preceded by an increase in ROS. We further showed that DMBA-induced apoptosis is associated with increased numbers of BAX and activated caspase-3 immunopositive GCs and TCs. Treatment with the cell-permeable GSH analog GEE prevented the induction of apoptosis by DMBA. Depletion of

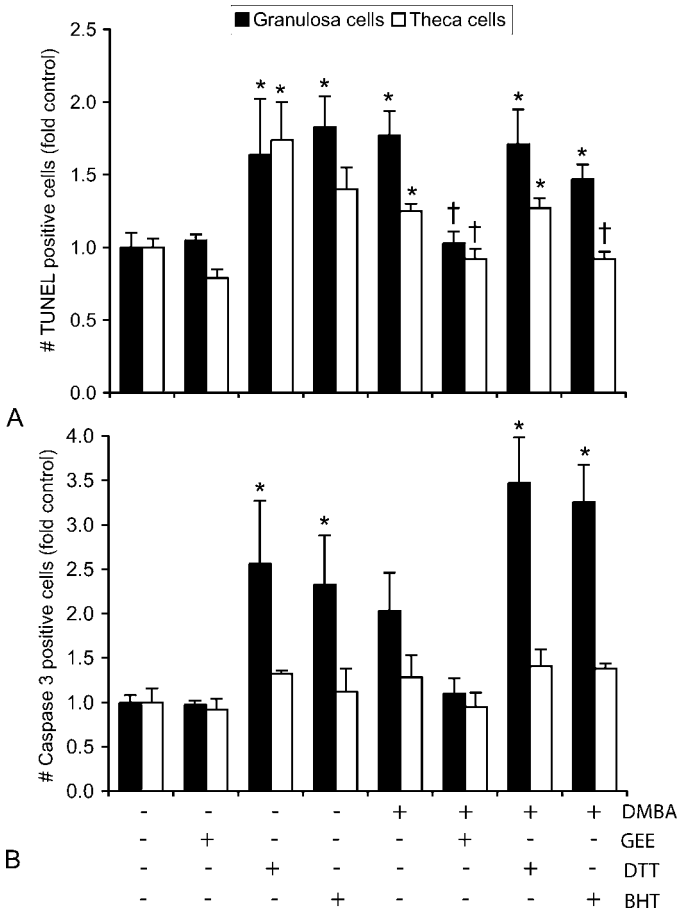

FIG. 4. Supplementation of GSH, but not of DTT or BHT, protects against DMBA-induced apoptosis. Preovulatory follicles were cultured for 48 h. All follicles were treated with 75 ng/ml FSH; some groups were treated with 10 μM DMBA and/or one of three antioxidants: 5 mM GEE, 0.5 mM DTT, or 0.2 mM BHT, as indicated on the graph. Apoptosis was assessed by TUNEL and activated caspase-3 immunostaining. **A**) Mean + SEM number of TUNEL-positive granulosa cells (GCs) or theca cells (TCs) per ×400 field expressed as fold the FSH-treated control value. There was a statistically significant effect of treatment on both GCs and TCs by one-way ANOVA ($P = 0.002$ and $P < 0.001$, respectively). *, Significantly different from FSH by the LSD test at $P < 0.05$; †, significantly different from FSH+DMBA by the LSD test at $P < 0.05$. $N = 3$–8 follicles/group. **B**) Mean + SEM number of activated caspase-3-positive GCs or TCs per ×400 field. There was a statistically significant effect of treatment on activated caspase-3 in GCs by the Kruskal-Wallis test ($P = 0.001$). *, Significantly different from FSH by the Mann-Whitney test at $P < 0.05$. $N = 3$–7 follicles/group.

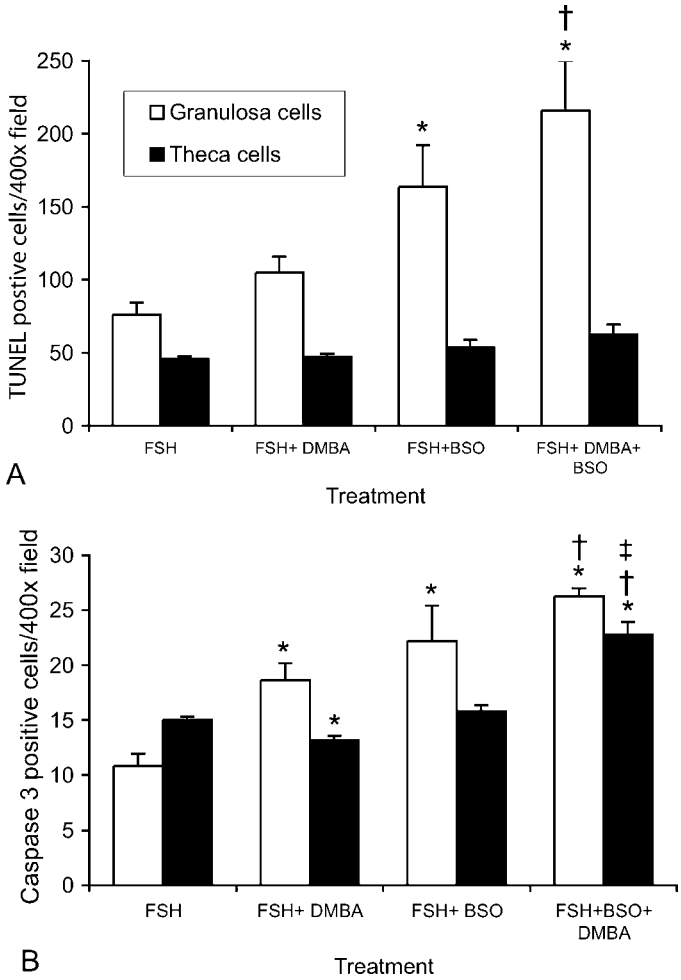

FIG. 5. Depletion of follicular GSH potentiates the induction of granulosa cell apoptosis by DMBA. Preovulatory follicles were cultured with 75 ng/ml FSH with or without 100 μM BSO for 8 h to deplete GSH. After 8 h, DMBA dissolved in DMSO or an equal volume of DMSO alone was added to the culture media for a final concentration of 0.5 μM DMBA, and follicles were cultured for an additional 40 h. Follicles were then processed for detection of apoptosis by TUNEL or activated caspase-3 immunostaining. **A**) Mean + SEM number of TUNEL-positive granulosa cells or theca cells per ×400 field. The effect of treatment on granulosa cell apoptosis was statistically significant ($P = 0.002$ by the Kruskal-Wallis test). **B**) Mean + SEM number of activated caspase-3-positive granulosa cells or theca cells per ×400 field. The effects of treatment on granulosa cell and theca cell apoptosis were statistically significant ($P = 0.004$ and $P = 0.002$, respectively, by the Kruskal-Wallis test). *, Significantly different from FSH; †, significantly different from FSH+DMBA; ‡, significantly different from FSH+BSO by the Mann-Whitney test at $P < 0.05$.

GSH with BSO enhanced the apoptotic effect of DMBA on apoptosis in cultured follicles. These latter two findings demonstrate the importance of GSH in protecting against DMBA-induced follicular toxicity.

The mechanisms by which PAHs induce apoptosis have been investigated in several systems. Treatment of immature mice with DMBA or of cultured neonatal mouse ovaries with the dihydrodiol metabolite of DMBA led to increased expression of BAX protein in oocytes of primordial follicles via increased transcription of *Bax* and subsequent destruction of primordial follicles [35]. This upregulation of BAX and destruction of primordial follicles was inhibited by AHR receptor antagonists and did not occur in *Ahr*-deficient or *Bax*-deficient mice [35]. Moreover, evidence was presented that functional arylhydrocarbon response elements in the *Bax* promoter were required for the upregulation of *Bax* transcription in oocytes [35]. *Bax* and *Ahr* also appear to be required for the induction of apoptosis by PAHs in murine embryos [48]. In the present study, we also observed increasing BAX protein expression with DMBA treatment in GCs and TCs at 24 h, prior to the increase in TUNEL-positive cells (Fig. 1). Moreover, our observations that DMBA treatment causes ROS generation prior to the onset of apoptosis (Figs. 1 and 3) suggest a mechanism for BAX activation by DMBA in antral follicles. Oxidative stress has recently been shown to induce BAX translocation to the mitochondria, resulting in cytochrome c release [49]. Moreover, the PAH BaP induced BAX translocation to the mitochondria without increasing overall levels of BAX protein in Hepa1c1c7 cells [50].

The present study also supports a role for caspase-3 in mediating DMBA-induced follicular apoptosis, as numbers of

activated caspase-3-positive GCs and TCs increased in concentration-dependent manner with DMBA treatment (Fig. 1). Activation of caspase-3 has been shown to be necessary for the induction of apoptosis by DMBA in bone marrow B cells [51]. Caspase-3 activation has also been implicated in the induction of apoptosis in Hepa1c1c7 cells by BaP [50]. All the apoptotic markers we assessed increased with a similar time course in GCs and TCs, suggesting that apoptosis of both cell types in concert drives the induction of antral follicle atresia by DMBA. It is also possible that apoptosis of one or the other cell type occurs first, between the 12- and 24-h time points that we assessed. Our study was not designed to investigate the effects of DMBA on the oocyte; however, we did not observe oocyte TUNEL or activated caspase-3 staining with DMBA treatment (data not shown). DMBA treatment also did not appear to increase BAX immunostaining in oocytes, with the exception of two oocytes in the 100 μM group at 48 h (data not shown). The endogenous process of antral follicle atresia is thought to be driven by GC apoptosis in vivo [34]. An early study of the effects of PAHs on follicular atresia in vivo described the destruction of somatic cells of large follicles occurring by 4 days after DMBA treatment, but no mention was made of whether GC or TC demise was more pronounced or had occurred earlier [6]. We are not aware of any other studies that examined the effects of PAHs on GCs and TCs of antral follicles.

PAHs require metabolic activation to reactive metabolites to exert their toxicity [18]. Therefore, our observation that DMBA induced apoptosis in cultured preovulatory follicles shows that these follicles are capable of metabolizing DMBA. This is consistent with previous studies, which showed that the major enzymes involved in PAH metabolism, CYP1A1, CYP1B1, microsomal epoxide hydrolase, and dihydrodiol dehydrogenase, are all expressed in rodent ovaries [52–56] and that cultured GCs obtained from preovulatory rat follicles are capable of metabolizing DMBA and BaP [57, 58]. Metabolism of PAHs begins with oxidation to arene oxides, which can be hydrolyzed to dihydrodiols. The dihydrodiols can be further oxidized to diol epoxides [13, 14]. A recent study showed that concentrations of another PAH, BaP, in culture medium decreased by about 30% within the first 30 min of being placed in polystyrene tissue culture plates due to binding to the plastic; however, a similar decline was not observed in polypropylene tubes [59]. Our follicles were cultured in glass scintillation vials, and binding of DMBA to the vials was likely low. The study by Kushman et al. [59] also showed that BaP was metabolized in the presence of cells expressing CYP1A1. From 30 min to 48 h, the amount of BaP per plate declined by 98% in plates with the CYP1A1-expressing cell line, while the concentration of the diol epoxide metabolite of BaP peaked at 24 h and then declined. In contrast, BaP declined by only 65% in the plates with the non-CYP1A1-expressing cells, and diol epoxide levels remained very low throughout the culture period. A similar decline in DMBA and increase in its metabolites likely occurred during the course of the culture period in our experiment.

The diol epoxide metabolites of PAHs are highly reactive and rapidly form DNA adducts [18]. A diol epoxide metabolite of BaP had a greater than 10-fold lower median effective dose for primordial and primary follicle destruction than BaP or than the parent dihydrodiol metabolite after intraovarian injection, and it was concluded that diol epoxides were therefore the ultimate ovotoxicants [17]. The dihydrodiol metabolites of PAHs can alternatively be oxidized by members of the aldo-keto reductase superfamily, the dihydrodiol dehydrogenases, to ketols, which tautomerize to catechols. The catechols undergo oxidation first to an *o*-semi-quinone anion radical and hydrogen peroxide and then to an *o*-quinone and superoxide anion [18]. Redox cycling can occur when the *o*-quinone undergoes either one or two electron reductions back to *o*-semiquinone or to catechol, respectively [18]. Treatment of cultured cells with BaP quinones has been shown to induce ROS formation [19], and oxidative DNA damage has been reported upon in vitro exposure of DNA to PAH quinones [18, 60]. DMBA treatment in vivo caused accumulation of lipid peroxidation products in intestinal mucosa [61] and in liver and erythrocytes [62]. Our observation of increased generation of ROS in preovulatory follicles cultured with DMBA prior to the onset of apoptosis and rescue of the follicles from DMBA-induced apoptosis by GSH supplementation with GEE suggests that ROS mediate DMBA-induced apoptosis in these follicles. The lack of a protective effect of two other antioxidants, DTT and BHT, is not necessarily inconsistent with this conclusion. BHT and DTT react with ROS and protect against induction of apoptosis in some cell systems [41, 63] but exert proapoptotic and prooxidant effects in other systems [64, 65]. Our results show that both of these agents are proapoptotic in preovulatory follicles.

In vivo administration of DMBA depressed GSH concentrations in intestinal mucosa, liver, and blood [61, 62]. Treatment of peripheral blood lymphocytes for 6 h with BaP 7,8-diol-9,10-epoxide, BaP 4,5-epoxide, and 7-OH-BaP, but not with BaP, DMBA, or BaP dihydrodiol, caused a decline in intracellular GSH concentrations [66]. We observed no decline in total GSH concentrations or any statistically significant effect on rGSH or GSSG concentrations in cultured preovulatory follicles treated with DMBA in the present study (Fig. 2), despite evidence that DMBA is metabolized in these cultured follicles. Our observations that enhancement of intracellular GSH concentrations with GEE prevented DMBA-induced GC and TC apoptosis (Fig. 4) and that depletion of GSH enhanced DMBA-induced apoptosis (Fig. 5) show that variations in intracellular GSH synthesis modify susceptibility to PAH-induced follicular toxicity. This is relevant to humans because polymorphisms have been identified in the promoters of both subunits of glutamate cysteine ligase, the rate-limiting enzyme in GSH synthesis that affects basal and/or inducible GSH synthesis [67–69].

The present study shows that DMBA induces apoptosis in GCs and TCs of cultured preovulatory follicles. The data suggest that DMBA treatment results in the generation of ROS, which leads to increased levels of the proapoptotic protein BAX, caspase-3 activation, and ultimately cell death. The observations that 1) the depletion of the antioxidant GSH potentiates the proapoptotic effect of DMBA and 2) GSH supplementation abolishes the proapoptotic effect of DMBA in cultured preovulatory follicles further support the hypothesis that ROS mediate DMBA-induced apoptosis. The results also demonstrate the important role of GSH in protecting follicles from toxicant-induced apoptosis.

ACKNOWLEDGMENT

We thank Dr. Zifu Wang, Manager of the University of California Irvine Microscopy and Image Analysis Facility, for his expert assistance with the confocal microscopy.

REFERENCES

1. Agency for Toxic Substances and Disease Registry. Toxicological Profile for Polycyclic Aromatic Hydrocarbons. Atlanta: U.S. Department of Health and Human Services, Public Health Service, Agency for Toxic Substances and Disease Registry; 1995.
2. Jongeneelen FJ, Anzion RBM, Leijdekkers C-M, Bos RP, Henderson PT.

1-Hydroxypyrene in human urine after exposure to coal tar and a coal tar derived product. Int Arch Occup Environ Health 1985; 57:47–55.
3. Menzie CA, Potocki BB, Santodonato J. Ambient concentrations and exposure to carcinogenic PAHs in the environment. Environ Sci Technol 1992; 26:1278–1284.
4. Borman SM, Christian PJ, Sipes IG, Hoyer PB. Ovotoxicity in female Fischer rats and B6 mice induced by low-dose exposure to three polycyclic aromatic hydrocarbons: comparison through calculation of an ovotoxic index. Toxicol Appl Pharmacol 2000; 167:191–198.
5. Mattison DR. Difference in sensitivity of rat and mouse primordial oocytes to destruction by polycyclic aromatic hydrocarbons. Chem Biol Interact 1979; 28:133–137.
6. Mattison DR. Morphology of oocyte and follicle destruction by polycyclic aromatic hydrocarbons in mice. Toxicol Appl Pharmacol 1980; 53:249–259.
7. Mattison DR, Nightingale MS. Oocyte destruction by polycyclic aromatic hydrocarbons is not linked to the inducibility of ovarian aryl hydrocarbon (benzo(a)pyrene) hydroxylase activity in (DBA/2N × C57BL/6N) F1 × DBA/2N backcross mice. Pediatr Pharmacol 1982; 2:11–21.
8. Mattison DR, Plowchalk DR, Meadows MJ, Miller MM, Malek A, London S. The effect of smoking on oogenesis, fertilization, and implantation. Semin Reprod Endocrinol 1989; 7:291–304.
9. Harlow BL, Signorello LB. Factors associated with early menopause. Maturitas 2000; 35:3–9.
10. Alderete E, Eskenazi B, Sholtz R. Effect of cigarette smoking and coffee drinking on time to conception. Epidemiology 1995; 6:403–408.
11. Baird DD, Wilcox AJ. Cigarette smoking associated with delayed conception. JAMA 1985; 253:2979–2983.
12. Swartz WJ, Mattison DR. Benzo(a)pyrene inhibits ovulation in C57BL/6N mice. Anat Rec 1985; 212:268–276.
13. Kleiner HE, Vulimiri S, Hatten WB, Reed MJ, Nebert DW, Jefcoate CR, DiGiovanni J. Role of cytochrome P4501 family members in the metabolic activation of polycyclic aromatic hydrocarbons in mouse epidermis. Chem Res Toxicol 2004; 17:1667–1674.
14. Shimada T, Fujii-Kuriyama Y. Metabolic activation of polycyclic aromatic hydrocarbons to carcinogens by cytochromes P450 1A1 and 1B1. Cancer Sci 2004; 95:1–6.
15. Denissenko MF, Pao A, Tang M-S, Pfeifer GP. Preferential formation of benzo[a]pyrene adducts at lung cancer mutational hotspots in P53. Science 1996; 274:430–432.
16. Wood AW, Chang RL, Levin W, Thomas PE, Ryan D, Stoming TA, Thakker DR, Jerina DM, Conney AH. Metabolic activation of 3-methylcholanthrene and its metabolites to products mutagenic to bacterial and mammalian cells. Cancer Res 1978; 38:3398–3404.
17. Takizawa K, Yagi H, Jerina DM, Mattison DR. Murine strain differences in ovotoxicity following intraovarian injection with benzo(*a*)pyrene, (+)-(7*R*,8*S*)-oxide, (-)-(7*R*,8*S*)-dihydrodiol, or (+)-(7*R*,8*S*)-diol-(9*S*,10*R*)-epoxide-2. Cancer Res 1984; 44:2571–2576.
18. Xue W, Warshawsky D. Metabolic activation of polycyclic aromatic hydrocarbon and heterocyclic aromatic hydrocarbons and DNA damage: a review. Toxicol Appl Pharmacol 2005; 206:73–93.
19. Reed MD, Monske ML, Lauer FT, Meserole SP, Born JL, Burchiel SW. Benzo[a]pyrene diones are produced by photochemical and enzymatic oxidation and induce concentration-dependent decreases in the proliferative state of human pulmonary epithelial cells. J Toxicol Environ Health, Part A 2003; 66:1189–1205.
20. Dalton TP, Chen Y, Schneider SN, Nebert DW, Shertzer HG. Genetically altered mice to evaluate glutathione homeostasis in health and disease. Free Radic Biol Med 2004; 37:1511–1526.
21. Jernström B, Funk M, Frank H, Mannervik B, Seidel A. Glutathione-*S*-transferase A1–1-catalysed conjugation of bay and fjord region diol epoxides of polycyclic aromatic hydrocarbons with glutathione. Carcinogenesis 1996; 17:1491–1498.
22. Romert L, Dock L, Jenssen D, Jernström B. Effects of glutathione transferase activity on benzo[a]pyrene 7,8-dihydrodiol metabolism and mutagenesis studied in a mammalian cell co-cultivation assay. Cancer Res 1989; 10:1701–1707.
23. Seidel A, Friedberg T, Löllman B, Schwierzok A, Funk M, Frank H, Holler R, Oesch F, Glatt H. Detoxification of optically active bay- and bjord-region polycyclic aromatic hydrocarbon dihydrodiol epoxides by human glutathione transferase P1–1 expressed in Chinese hamster V79 cells. Carcinogenesis 1998; 19:1975–1981.
24. Lopez SG, Luderer U. Effects of cyclophosphamide and buthionine sulfoximine on ovarian glutathione and apoptosis. Free Radic Biol Med 2004; 36:1366–1377.
25. Mattison DR, Shiromizu K, Pendergrass JA, Thorgeirsson SS. Ontogeny of ovarian glutathione and sensitivity to primordial oocyte destruction by cyclophosphamide. Pediatr Pharmacol 1983; 3:49–55.
26. Calvin HI, Grosshans K, Blake EJ. Estimation and manipulation of glutathione levels in prepuberal mouse ovaries and ova: relevance to sperm nucleus transformation in the fertilized egg. Gamete Res 1986; 14: 265–275.
27. Perreault SD, Barber RR, Slott VL. Importance of glutathione in the acquisition and maintenance of sperm nuclear decondensing activity in maturing hamster oocytes. Dev Biol 1988; 125:181–186.
28. Sutovsky P, Schatten G. Depletion of glutathione during bovine oocyte maturation reversibly blocks the decondensation of the male pronucleus and pronuclear apposition during fertilization. Biol Reprod 1997; 56: 1503–1512.
29. Zuelke KA, Jones DP, Perreault SD. Glutathione oxidation is associated with altered microtubule function and disrupted fertilization in mature hamster oocytes. Biol Reprod 1997; 57:1413–1419.
30. Luderer U, Kavanagh TJ, White CC, Faustman EM. Gonadotropin regulation of glutathione synthesis in the rat ovary. Reprod Toxicol 2001; 15:495–504.
31. Tsai-Turton M, Luderer U. Gonadotropin regulation of glutamate cysteine ligase catalytic and modifier subunit expression in the rat ovary is subunit and follicle stage-specific. Am J Physiol 2005; 289:E391–E402.
32. Luderer U, Diaz D, Faustman EM, Kavanagh TJ. Localization of glutamate cysteine ligase subunit mRNA within the rat ovary and relationship to follicular atresia. Mol Reprod Dev 2003; 65:254–261.
33. Tsai-Turton M, Luderer U. Opposing effects of glutathione depletion and FSH on reactive oxygen species and apoptosis in cultured preovulatory rat follicles. Endocrinology 2006; 147:1224–1236.
34. Tilly JL, Robles R. Apoptosis and its impact in clinical reproductive medicine. In: Fauser BCJM, Rutherford AJ, Strauss JF III, Van Steirteghem A (eds.), Molecular Biology in Reproductive Medicine. New York: Parthenon; 1999:79–101.
35. Matikainen T, Perez GI, Jurisicova A, Pru JK, Schlezinger JJ, Ryu H-Y, Laine J, Sakai T, Korsmeyer SJ, Casper RF, Sherr DH, Tilly JL. Aromatic hydrocarbon receptor-driven Bax gene expression is required for premature ovarian failure caused by biohazardous environmental chemicals. Nat Genet 2001; 28:355–360.
36. Tilly JL, Billig H, Kowalski KI, Hsueh AJW. Epidermal growth factor and basic fibroblast growth factor suppress the spontaneous onset of apoptosis in cultured rat ovarian granulosa cells and follicles by a tyrosine kinase-dependent mechanism. Mol Endocrinol 1992; 6:1942–1950.
37. Tsafriri A, Lindner HR, Zor U, Lamprecht SA. In-vitro induction of meiotic division in follicle-enclosed rat oocytes by LH, cyclic AMP and prostaglandin E_2. J Reprod Fertil 1972; 31:39–50.
38. Griffith OW. Mechanism of action, metabolism, and toxicity of buthionine sulfoximine and its higher homologs, potent inhibitors of glutathione synthesis. J Biol Chem 1982; 257:13704–13712.
39. Puri RN, Meister A. Transport of glutathione as γ-glutamylcysteinylglycyl ester into liver and kidney. Proc Natl Acad Sci U S A 1983; 80:5258–5260.
40. Armstrong JS, Steinauer KK, Hornung B, Irish JM, Lecane P, Birrell GW, Peehl DM, Knox SJ. Role of glutathione depletion and reactive oxygen species generation in apoptotic signaling in a human B lymphoma cell line. Cell Death Differ 2002; 9:252–263.
41. Yue P, Zhou Z, Khuri FR, Sun S-Y. Depletion of intracellular glutathione contributes to JNK-mediated death receptor 5 upregulation and apoptosis by the novel synthetic triterpinoid methyl-2-cyano-3,12dioxoolean-1,9-dien-28-oate (CDDO-Me). Cancer Biol Ther 2006; 5:492–497.
42. Hansen JM, Lee E, Harris C. Spatial activities and induction of glutamate-cysteine ligase (GCL) in the postimplantation rat embryo and visceral yolk sac. Toxicol Sci 2004; 81:371–378.
43. Griffith OW. Determination of glutathione and glutathione disulfide using glutathione reductase and 2-vinylpyridine. Anal Biochem 1980; 106: 207–212.
44. Chun S-Y, Billig H, Tilly JL, Furuta I, Tsafriri A, Hsueh AJW. Gonadotropin suppression of apoptosis in cultured preovulatory follicles: mediatory role of endogenous insulin-like growth factor I. Endocrinology 1994; 135:1845–1853.
45. Yacobi K, Wojtowicz A, Tsafriri A, Gross A. Gonadotropins enhance caspase-3 and −7 activity and apoptosis in the theca-interna cells of rat preovulatory follicles in culture. Endocrinology 2004; 145:1943–1951.
46. Rothe G, Emmendorffer A, Oser A, Roseler J, Valet G. Flow cytometric measurement of the respiratory burst activity of phagocytes using dihydrorhodamine123. J Immunol Methods 1991; 138:133–135.
47. Royall JA, Ischiropoulos H. Evaluation of 2′,7′-dichlorofluorescein and dihydrorhodamine 123 as fluorescent probes for intracellular H_2O_2 in cultured endothelial cells. Arch Biochem Biophys 1993; 302:348–355.
48. Detmar J, Rabaglino T, Taniuchi Y, Oh J, Acton BM, Benito A, Nunez G,

Jurisicova A. Embryonic loss due to exposure to polycyclic aromatic hydrocarbons is mediated by Bax. Apoptosis 2006; 11:1413–1425.
49. D'Alessio M, De Nicola M, Coppola S, Gualandi G, Pugliese L, Cerella C, Cristofanon S, Civitareale P, Ciriolo MR, Bergamaschi A, Magrini A, Ghibelli L. Oxidative Bax dimerization promotes its translocation to mitochondria independently of apoptosis. FASEB J 2005; 19:1504–1506.
50. Solhaug A, Refsnes M, Låg M, Schwarze PE, Husøy T, Holme JA. Polycyclic aromatic hydrocarbons induce both apoptotic and anti-apoptotic signals in Hepa1c1c7 cells. Carcinogenesis 2004; 25:809–819.
51. Ryu H-Y, Emberley JK, Schlezinger JJ, Allan LL, Na S, Sherr DH. Environmental chemical-induced bone marrow B cell apoptosis: death receptor-independent activation of a caspase-3 to caspase-8 pathway. Mol Pharmacol 2005; 68:1087–1096.
52. Bhattacharyya KK, Brake PB, Eltom SE, Otto SA, Jefcoate CR. Identification of a rat adrenal cytochrome P450 active in polycyclic aromatic hydrocarbon metabolism as rat CYP1B1. J Biol Chem 1995; 270:11595–11602.
53. Hou Y-T, Xia W, Pawlowski JE, Penning TM. Rat dihydrodiol dehydrogenase: complexity of gene structure and tissue-specific and sexually dimorphic gene expression. Cancer Res 1994; 54:247–255.
54. Shimada T, Sugie A, Shindo M, Nakajima T, Azuma E, Hashimoto M, Inoue K. Tissue-specific induction of cytochromes P450 1A1 and 1B1 by polycyclic aromatic hydrocarbons and polychlorinated biphenyls in engineered C57BL/6J mice of *Arylhydrocarbon receptor* gene. Toxicol Appl Pharmacol 2003; 187:1–10.
55. Springer LN, Tilly JL, Sipes IG, Hoyer PB. Enhanced expression of Bax in small preantral follicles during 4-vinylcyclohexene diepoxide-induced ovotoxicity in the rat. Toxicol Appl Pharmacol 1996; 139:402–410.
56. Otto S, Bhattacharyya KK, Jefcoate CR. Polycyclic aromatic hydrocarbon metabolism in rat adrenal, ovary, and testis microsomes is catalyzed by the same novel cytochrome P450 (P450RAP). Endocrinology 1992; 131: 3067–3076.
57. Becedas L, Romert L, Toft E, Jenssen D, DePierre JW, Ahlberg MB. Metabolism of polycyclic aromatic hydrocarbons to mutagenic species by rat and porcine ovarian granulosa cells: detection by cocultivation with V79 Chinese hamster cells. Reprod Toxicol 1993; 7:219–224.
58. Bengtsson M, Reinholt FP, Rydström J. 7,12-Dimethylbenz[a]anthracene mono-oxygenase activity in the rat ovary. Toxicology 1992; 71.
59. Kushman ME, Kabler SL, Fleming MH, Ravoori S, Gupta RC, Doehmer J, Morrow CS, Townsend AJ. Expression of human glutathione *S*-transferase P1 confers resistance to benzo[a]pyrene or benzo[a]pyrene-7,8-dihydrodiol mutagenesis, macromolecular alkylation and formation of stable N2-Gua-BPDE adducts in stably transfected V79MZ cells co-expressing hCYP1A1. Carcinogenesis 2007; 28:207–214.
60. Seike K, Murata M, Oikawa S, Hiraku Y, Hirakawa K, Kawanishi S. Oxidative DNA damage induced by ben[a]anthracene metabolites via redox cycle of quinone and unique non-quinone. Chem Res Toxicol 2003; 16:1470–1476.
61. Khajuria A, Thusu N, Zutshi U, Bedi KL. Piperine modulation of carcinogen induced oxidative stress in intestinal mucosa. Mol Cell Biochem 1998; 189:113–118.
62. Chandra Mohan KVP, Abraham SK, Nagini S. Protective effects of a mixture of dietary agents against 7,12-dimethylbenz[a]anthracene-induced genotoxicity and oxidative stress in mice. J Med Food 2004; 7:55–60.
63. Festjens N, Kalai M, Smet J, Meeus A, Van Coster R, Saelens X, Vandenabeele P. Butylated hydroxyanisole is more than a reactive oxygen species scavenger. Cell Death Differ 2006; 13:166–169.
64. Anderson KM, Ou D, Wu YB, Jajeh A, Harris JE. Induction of type 1 programmed cell death in U937 cells by the antioxidant, butylated hydroxy-toluene or the free radical spin trap, NTBN. Leuk Res 1999; 23: 665–673.
65. Tartier L, McCarey YL, Biaglow JE, Kochevar IE, Held KD. Apoptosis induced by dithiothreitol in HL-60 cells shows early activation of caspase 3 and is independent of mitochondria. Cell Death Differ 2000; 7:1002–1010.
66. Romero DL, Mounho BJ, Lauer FT, Born JL, Burchiel SW. Depletion of glutathione by benzo(a)pyrene metabolites, ionomycin, thapsigargin, and phorbol myristate in human peripheral blood mononuclear cells. Toxicol Appl Pharmacol 1997; 144:62–69.
67. Nakamura S-I, Kugiyama K, Sugiyama S, Miyamoto S, Koide S-I, Fukushima H, Honda O, Yoshimura M, Ogawa H. Polymorphism in the 5'-flanking region of the human glutamate-cysteine ligase modifier subunit gene is associated with myocardial infarction. Circulation 2002; 105:2968–2973.
68. Walsh AC, Feulner JA, Reilly A. Evidence for functionally significant polymorphism of human glutamate cysteine ligase catalytic subunit: association with glutathione levels and drug resistance in the National Cancer Institute Tumor Cell Line Panel. Toxicol Sci 2001; 61:218–223.
69. Koide S-I, Kugiyama K, Sugiyama S, Nakamura S-I, Fukushima H, Honda O, Yoshimura M, Ogawa H. Association of polymorphism in glutamate-cysteine ligase catalytic subunit gene with coronary vasomotor dysfunction and myocardial infarction. J Am Coll Cardiol 2003; 41: 539–545.